Augmentation of thermohydraulic performance in a dimpled tube using ternary hybrid nanofluid

Orhan Keklikcioglu[1]*

[1]Department of Mechanical Engineering, Faculty of Engineering, Erciyes University, Turkey

Orcid: O. Keklikcioglu (0000-0002-6227-3130)

Abstract: This computational study explores the thermal and hydraulic efficiency of heat exchanger tube configurations utilizing hybrid nanofluids and circular dimples. Seven distinct configurations incorporating different volumetric concentrations of three nanoparticles (GnP, MWCNT, and Fe_3O_4) and two circular dimple pitch ratios are examined. The investigation concentrates on crucial parameters, including Nusselt number, friction factor, and thermohydraulic performance. The numerical analysis specifically addresses single-phase flow within the Reynolds number range of 5000-30000, maintaining a constant surface heat flux during simulations. Notably, Nusselt number consistently rises with Reynolds number across all configurations. Friction factor analysis indicates minimal sensitivity to hybrid nanofluid ratios but an increase with circular dimples. Despite the elevated pressure drop, the thermohydraulic coefficient consistently surpasses 1, signifying a net energy gain from enhanced heat transfer. Optimal performance is observed in the S5-P/Dt=1 configuration, exhibiting the highest thermohydraulic coefficient at 1.35, while the P/Dt =2 variation within the same fluid model presents a slightly lower value of 1.32.

Keywords: Hybrid nanofluid, heat transfer enhancement, circular dimple, thermohydraulic performance.

1. Introduction

Improving the efficiency of cooling and heating systems can be achieved by enhancing heat transfer. Research on the enhancement of heat transfer is essential to reduce energy losses in the increasing energy demand in the current century [1-2].

In general, inserts are placed in the flow passage to enhance the heat transfer rate, resulting in a reduction in the hydraulic diameter of the flow passage [3]. Heat transfer enhancement consists of two different techniques, active and passive. Heat transfer enhancement in active methods requires external inputs such as electrostatic fields, mechanical vibration, or pulsation [4]. Passive methods deal with surface shape modifications or intensify the flow turbulence to enhance the heat transfer [5,6]. Porous materials [7-9], corrugated surfaces [10-13], extended surfaces [14-16], dimples [17-21], inserts such as wire coils, swirl flow tools, protrusions [22-25], and nanofluids [26-28] are some examples of passive techniques.

Considering the thermal-hydraulic performance, it becomes clear how significant the passive method is. In industries, improving thermal contact and reducing pumping power are crucial in terms of efficiency and economy to design better heat exchangers. The studies in the literature about passive methods show significant results

in thermal-hydraulic performance. Vicente et al. [29,30] presented that roughness has a powerful impact on the enhancement of thermal performance and, energy efficiency in their two studies with dimpled tubes and corrugated tubes, respectively. Zheng et al. [31] represented that the appliance of the inclined grooved tube enhances the heat transfer and friction factor (f) in the range of approximately 1.23 - 2.17 and 1.02 - 3.75 compared to smooth tubes, respectively. Chen et al. [32] analyzed the comparison of six different oriented dimpled copper tubes with a smooth tube. In their study, they tried to find the best performance according to the geometrical configuration of dimples. The maximum performance improvement has been found in the largest value of the ratio of the depth of the dimple to the inner diameter, the pitch of the dimple, and the number of dimples longitudinally. The heat transfer coefficient has improved between 1.25 - 2.37 times at a constant Re. In addition, the increase in f is between 1.08 to 2.35 higher than the smooth tube. In their study, the exponential Reynolds number (Re) is between 0.883 and 0.934. Piper et al. [33] probed the dimpled surface to enhance the pillow-plate heat exchanger. They showed that a dimpled surface decreased the pressure drop by around 9%. Similarly, comparing the dimpled surface with a smooth surface, the mean heat transfer coefficient has improved by 2.2%, and thermo-hydraulic performance enhanced by 11.2%. Bi

et al. [34] used two different heat passive methods dimples, grooves, and fins to improve heat transfer in their studies. In their study, apart from these three methods, they also examined different geometric configurations to select the most effective dimple. They showed that at lower *Re* of *Re*<3323 grooves have the highest value of PEC of around 1.35. However, dimple surfaces will reach the best performance of heat transfer augmentation as the *Re* increases. Moreover, the geometrical configuration of dimples in the study shows that the heat transfer enhancement is easier when the dimples are deeper with a large diameter. Xie et al. [21] analyzed the effect of cross ellipsoidal dimples on heat transfer based on different structural parameters. They indicated that although Nusselt number (*Nu*) and *f* increase with the increase in the depth of the dimples, Performance Evaluation Criteria (PEC) decreases. Moreover, another parameter in the study shows that *Nu* is inversely proportional to pitch. Similarly, the largest PEC is obtained in the smallest pitch in this case. Similar to pitch, PEC is inversely proportional to the axis ratio. As a result of their study, they obtained the highest PEC as 1.58 at a constant *Re* of 5000 with the combination of three structural parameters. Corrugated surfaces, fins, and dimples provide heat transfer improvement up to some limits due to their low heat transfer performance. Using nanoparticles with these methods improves heat transfer augmentation. Kabeel et al. [35] examined the effect of nanoparticles on the corrugated surface in their study. They have used Al_2O_3 nanomaterial in the water-based fluid with different volumetric concentrations (1-4%). In the study, the heat transfer coefficient increased up to 13% after adding nanomaterial with a 4% concentration. Khairul et al. [36] showed that using nanofluid of CuO with the corrugated surface enhanced the heat transfer coefficient up to 24.7%. Firoozi et al. [26] numerically investigated the heat transfer characteristics of nanofluid in 27 configurations of the dimple. They achieved the highest PEC of 2.50 and 3.12 for water and the flow of Al_2O_3 nanofluid, respectively. Suresh et al. [37] experimentally showed that CuO/Water nanofluid enhanced the heat transfer coefficient 1.06 times and 1.15 times based on the concentration of the nanoparticles of 0.1% and 0.3% in the helically dimpled tube, respectively.

Recently, hybrid nanofluids are attracting more attention as a new heat transfer enhancement method. Hybrid nanofluid consists of two or more different nanoparticles. In the literature, it has been seen that hybrid nanofluids are more effective in improving heat transfer than monotype nanofluids [38]. There are several studies about hybrid nanofluids. Toghraie et al. [39] researched the effect of hybrid nanofluids on thermal conductivity. The study showed that $ZnO–TiO_2$ hybrid nanofluids in ethylene glycol enhanced the thermal conductivity by around 32%. Sundar et al. [40] experimentally observed that nanodiamond-nickel hybrid nanofluid in water base fluid enhanced the thermal conductivity and viscosity by around 29% and 23%, respectively compared to water. Moreover, the *Nu* enhancement is about 25% and 35% according to 0.1% and 0.3% volumetric concentration of hybrid nanofluid. Khan et al. [41] demonstrated that alumina/silica hybrid nanofluid achieved the maximum value of PEC as 1.24 in the mini channel heat sink. Ahmed et al. [42] numerically investigated the thermo-hydraulic performance of nanofluids in a dimpled channel. The result shows that the heat transfer coefficient is 35% for the dimpled channel and around 46%, 44%, and 42% for Al_2O_3, Al_2O_3-CuO, and CuO nanofluids, respectively.

As it can be seen that different configurations of dimples and different passive methods are used in the literature review. In addition, heat transfer enhancement was made by using these passive methods with the combination of different nanofluids. As seen in these studies, it is possible to improve heat transfer at certain rates with different configurations of different methods. In this study, seven different configurations of hybrid nanofluids are studied from different volumetric concentrations of three (GnP, MWCNT, Fe_3O_4) nanoparticles. The most effective configuration is tried to be obtained by analyzing these seven different hybrid nanofluids in a pipe with a dimpled surface. In addition, graphene, carbon nanotube, and iron oxide nanoparticles with different geometrical shapes are studied as nanoparticles. The addition of iron oxide to these hybrid nanofluids will also allow for thermal performance modification using active methods in the future.

2. Materials and Method

2.1. Numerical model

The objective of this research is to investigate the thermohydraulic performance of a dimpled tube using CFD software, considering different ternary nanofluid compositions. The solution domain for a dimpled tube is illustrated in Figure 1, while Table 1 outlines the physical parameters of the numerical model.
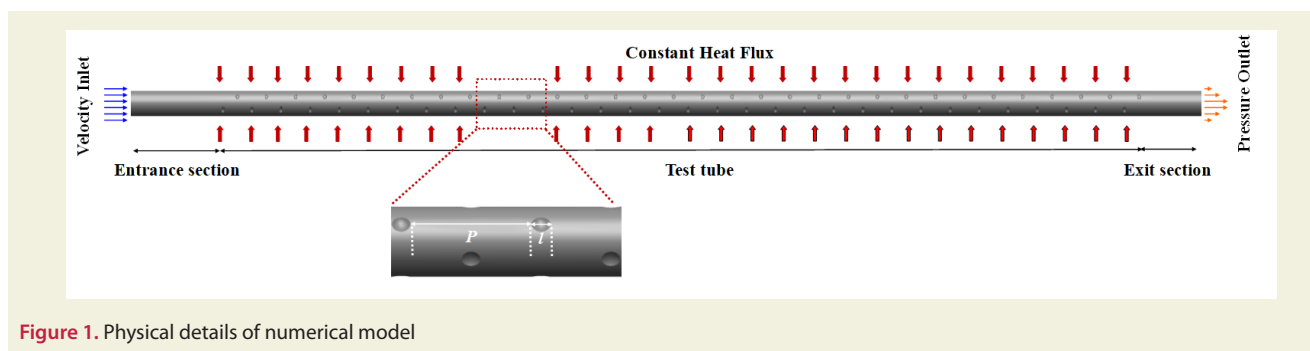

Figure 1. Physical details of numerical model

The numerical model consists of three sections: the inlet, the test, and the outlet. The inlet section generates flow hydrodynamically and prevents any disturbances at the entrance of the tube. The lengths of the inlet, test, and outlet sections are chosen to be 100 mm, 1000 mm, and 50 mm, respectively. The outer surface of the tube wall is exposed to a continuous heat flow of 20 kW/m². The investigation involves the use of ternary hybrid nanofluid configurations flowing through the tube with Re ranging from 5000 to 30000. The numerical analyses consider parameters such as the pitch ratio (P/D_t = 1 and 2) and nanoparticle loading fraction.

Table 1. Geometrical parameters of dimpled tube.

Geometric parameter	Value(mm)
Diameter of tube(D_t)	15
Length of entrance section(L_{ent})	100
Length of test tube(L_t)	1000
Length of exit section(L_{ex})	50
Length of dimple(l)	4
Height of dimple(h_d)	1.5
Pitch ratio (P/D_t)	1 and 2

2.2. Nanofluid configurations and thermophysical properties

In this study, the overall hybrid nanofluid volume ratio was set at 1.5%. The volumetric contribution levels of GnP, MWCNT, and FE_3O_4 nanoparticles, which compose the hybrid nanofluid, were varied within the range of 0.25-0.75% to establish seven distinct fluid configurations as given in Table 2.

Table 2. The volumetric contribution levels of nanoparticles

No	Volume fractions			
	GnP	MWCNT	FE_3O_4	Total
S1	0.0050	0.0050	0.0050	0.015
S2	0.0050	0.0075	0.0025	0.015
S3	0.0050	0.0025	0.0075	0.015
S4	0.0025	0.0050	0.0075	0.015
S5	0.0075	0.0050	0.0025	0.015
S6	0.0025	0.0075	0.0050	0.015
S7	0.0075	0.0025	0.0050	0.015

Table 3. Thermophysical properties of ternary hybrid nanofluid components[43]

Properties	Water	GnP	MWCNT	FE_3O_4
$\rho_{(kg/m^3)}$	998.2	2250	2100	5180
$C_{p(J/kg\,K)}$	4182	790	710	104
k (W/mK)	0.6	3000	2000	17.65

$$\mu_{Thnf} = \frac{\mu_f}{(1-\phi_1)^{2.5}(1-\phi_2)^{2.5}(1-\phi_3)^{2.5}} \quad (1)$$

$$\rho_{Thnf} = \big[(1-\phi_1)\{(1-\phi_2)[(1-\phi_3)\rho_f + \rho_3\phi_3] + \rho_2\phi_2\} + \rho_1\phi_1\big] \quad (2)$$

$$(\rho C_p)_{Thnf} = (1-\phi_1)\{(1-\phi_2)[(1-\phi_3)(\rho C_p)_f + (\rho C_p)_{s_3}\phi_3] + (\rho C_p)_{s_2}\phi_2\} + (\rho C_p)_{s_1}\phi_1 \quad (3)$$

$$\frac{k_{Thnf}}{k_{hnf}} = \frac{k_1 + 2k_{nf} - 2\phi_1(k_{nf} - k_1)}{k_1 + 2k_{nf} + \phi_1(k_{nf} - k_1)} \quad (4.a)$$

$$\frac{k_{hnf}}{k_{nf}} = \frac{k_2 + 2k_{nf} - 2\phi_2(k_{nf} - k_2)}{k_2 + 2k_{nf} + \phi_2(k_{nf} - k_2)} \quad (4.b)$$

$$\frac{k_{nf}}{k_f} = \frac{k_3 + 2k_{nf} - 2\phi_3(k_{nf} - k_3)}{k_3 + 2k_{nf} + \phi_3(k_{nf} - k_3)} \quad (4.c)$$

The unique thermophysical characteristics of three distinct nanoparticles and the base fluid (water), as outlined in Table 3, were utilized to calculate the viscosity, density, specific heat, and thermal conductivity of the ternary hybrid nanofluid using the Equations 1-4, respectively. Subsequently, the thermophysical properties of the seven different configurations were determined and subjected to further analysis.

2.3. Solution methodology

In this research, numerical analysis was conducted using the finite volume method in ANSYS Fluent 18. The turbulence model employed was the k - ε RNG (Re-Normalization Group), and the SIMPLE algorithm scheme was utilized to assess the correlation between pressure and velocity. For convection evaluation, the QUICK scheme was implemented. Convergence criteria for continuity, velocity, energy, k, and ε values were set at 1x10^{-5}. The k - ε RNG model, known for its precision among turbulence models, is based on three conservation equations of mass, momentum and energy, outlined in Equations 5, 6, and 7, respectively [44].

$$\nabla(\rho\vec{V}) = 0 \quad (5)$$

$$\nabla(\rho\vec{V}\vec{V}) = -\nabla P + \nabla(\mu\nabla\vec{V}) \quad (6)$$

$$\nabla(\rho c_p\vec{V}T) = \nabla(k\nabla T) \quad (7)$$

For the solution method RNG, the transport equations for k and ε are given in Equations 8 and 9, respectively.

$$\frac{\partial}{\partial t}(\rho k) + \frac{\partial}{\partial x_i}(\rho k u_i) = \frac{\partial}{\partial x_j}\left(\alpha_k \mu_{eff}\frac{\partial k}{\partial x_j}\right) + G_k + G_b - \rho\epsilon - Y_m + S_k \quad (8)$$

$$\frac{\partial}{\partial t}(\rho\epsilon) + \frac{\partial}{\partial x_i}(\rho\epsilon u_i) = \frac{\partial}{\partial x_j}\left(\alpha_\epsilon \mu_{eff}\frac{\partial\epsilon}{\partial x_j}\right) + C_{1\epsilon}\frac{\epsilon}{k}(G_k + C_{3\epsilon}G_b) - C_{2\epsilon}\rho\frac{\epsilon^2}{k} - R_\epsilon + S_\epsilon \quad (9)$$

Within these equations, G_k represents the production value of turbulent kinetic energy resulting from the velocity gradient, and G_b signifies the production value of turbulent kinetic energy arising from buoyancy. The parameters α_k and α_ε are defined as inverse effective Prandtl numbers for k and ε, respectively. Additionally, S_k and S_ε are characterized as user-input source data.

2.4. Data reduction

In addition to computing the thermophysical properties of the hybrid nanofluids, these properties were defined and analyzed using the ANSYS Fluent 18 program. The obtained data from the analysis were used to calculate the Re, Nu, f, and thermohydraulic performance coefficient based on the following equations. Specifically, the Re was determined using Equation 10.

$$Re = \frac{\rho D V}{\mu} \tag{10}$$

The convective heat transfer coefficient is determined using Equation 11, where q' represents the applied heat flux over the flow field, and ΔT denotes the temperature difference between the surface temperature of the flow field and the average temperature as the median of the inlet and the outlet fluid temperatures in the test tube.

$$h = \frac{q'}{\Delta T} \tag{11}$$

Following the computation of the heat convection coefficient, the Nu was determined using Equation 12.

$$Nu = \frac{hD}{k} \tag{12}$$

Yet another dimensionless parameter, the coefficient of friction, was computed using Equation 13.

$$f = \frac{\Delta P}{\frac{1}{2}\rho V^2 \frac{L}{D}} \tag{13}$$

The coefficient of thermohydraulic performance was calculated using Equation 14.

$$\eta = \left(Nu_{hnf}/Nu_b\right)\left(f_b/f_{hnf}\right)^{1/3} \tag{14}$$

3. Results and Discussion

3.1. Grid independence and validation of numerical methodology

To ensure the numerical results are independent of the number of cells, a grid independence study was conducted prior to the numerical analysis in this study. The impact of varying the number of cells on Nu and friction number at a Re of 5000 was investigated. The findings indicate that the deviation in Nu and f remained below 1% when the number of cells reached around 4.12 mil-
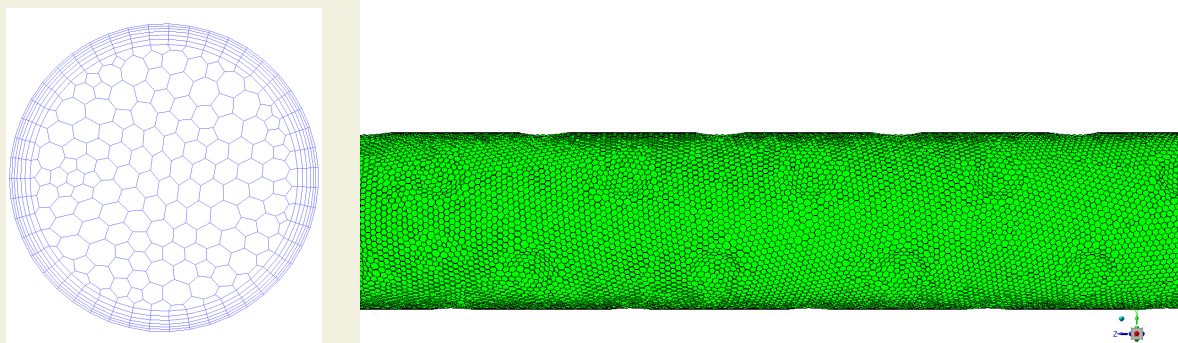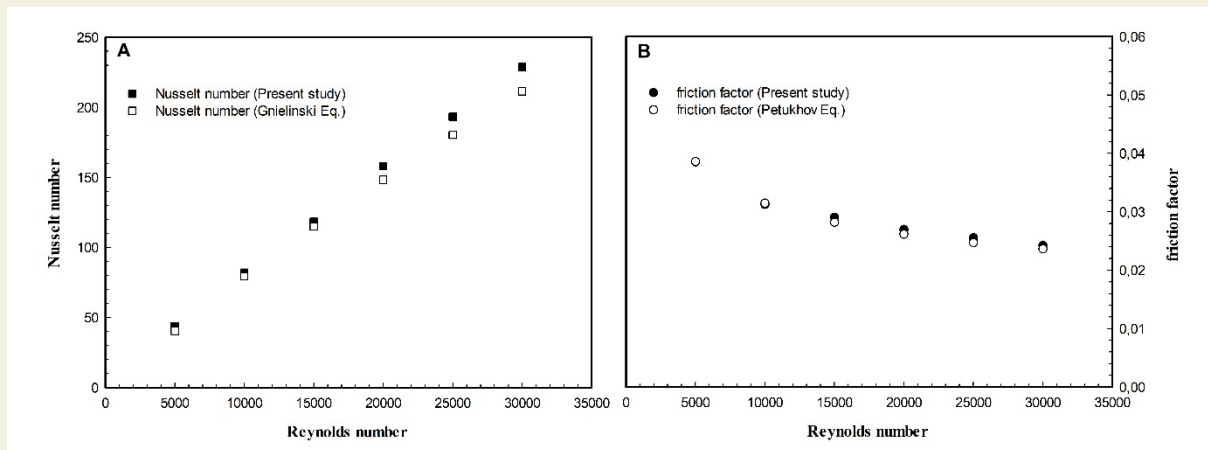

Figure 2. Grid structure of numerical model

Figure 3. Validation results of numerical procedure

lion. The parameter y⁺, crucial for controlling mesh models, was determined to be approximately $y^+ \approx 3$ within the boundary layer region, adhering to the condition $y+<5$ as required. Additionally, the skewness value of the mesh structure was found to be approximately ≈ 0.6, while the orthogonal quality value was approximately ≈ 0.4. Consequently, based on this result, the polyhedral grid structure depicted in Figure 2 was selected for further analysis.

In numerical investigations, it is essential to validate the outcomes of the analogy used for parameter evaluation by comparing them with established equations. In this study, the results obtained from the analysis using water fluid were validated with the equations provided by Gnielinski [45] and Petukhov [46] for Nu and f, respectively, as outlined in Equations 15 and 16.

$$Nu = \frac{(f/8)(Re_D - 1000)Pr}{1 + 12.7(f/8)^{1/2}(Pr^{2/3}-1)} \tag{15}$$

$$f = (0.79\ln(Re) - 1.64)^{-0.2} \tag{16}$$

As depicted in Figure 3, there is a remarkable agreement between the numerical results and established equations in the assessment of the Nu (Fig.3A) and f (Fig.3B). For the smooth heat exchanger tube utilizing water fluid, the highest observed error rates fall within the range of ±5.69% for the Nu and ±3.88% for the f.

3.2. Thermal and hydraulic characteristics

As illustrated in Figure 4, the Nu exhibited an ascending trend with the rise in Re across all configurations, aligning with expectations. The volumetric ratio of the hybrid nanofluid demonstrated a positive impact on the Nu, exhibiting an increase with the addition of the nano-additive. The incorporation of circular dimple once again resulted in enhanced heat transfer, and the Nu decreased as the distance between the dimples increased.

As depicted in Figure 4, the configuration S5-P/D_t=1 exhibited the most favorable thermal characteristics. The S5 fluid model comprises 0.75% GnP, 0.50% MWCNT, and 0.25% FE$_3$O$_4$, while maintaining the smallest variation in the distance between the circular dimples. In this analysis, it is substantiated that the fluid model with the highest thermal conductivity enhances thermal charac-
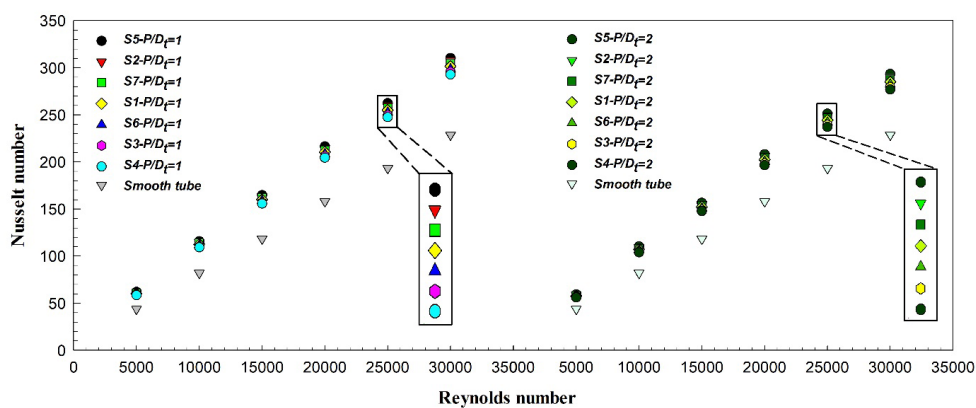

Figure 4. Distrubution of *Nu* versus *Re* for all configurations
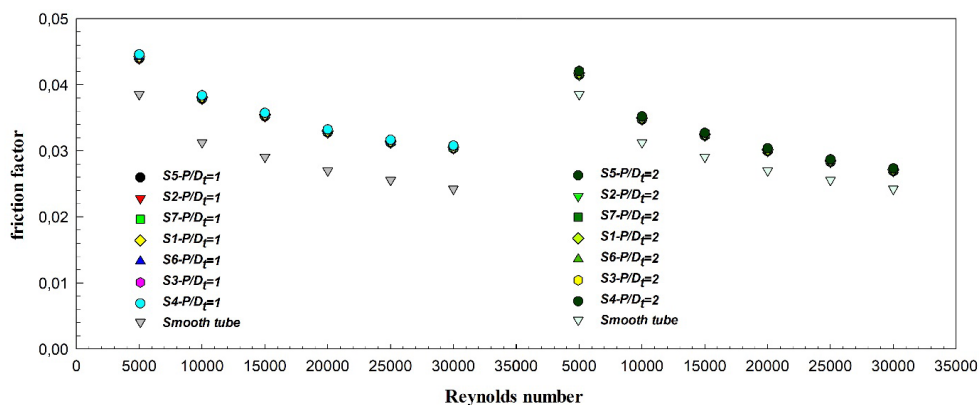

Figure 5. Distrubution of *f* versus *Re* for all configurations

teristics, and the implementation of a dimple model with a short distance is conducive to promoting turbulence.

Based on the obtained results, the S5-P/D_t=1 variation exhibited the highest Nu, reaching 61.87. This value is approximately 1.42 times higher than that of the smooth tube. In contrast, when the same fluid was used but with a P/D_t=2 variation, the Nu was slightly lower at 59.33. The lowest Nu, which was 56, occurred at P/D_t=2 for S4, representing the hybrid nanofluid model with the lowest thermal conductivity value.

As illustrated in Figure 5, the influence of hybrid nanofluid volumetric ratios on the friction coefficient appears to be quite limited. The coefficient of friction values remained approximately the same across different hybrid nanofluid mixing ratios. This consistency can be attributed to the fact that the total nanofluid volumetric ratios were consistent in all configurations.

The coefficient of friction showed an increase with the introduction of the circular dimple. Furthermore, there was a positive correlation between the coefficient of friction and the decreasing distance between the circular dimples. Conversely, a decreasing trend was observed in the coefficient of friction with an increase in Re.

Based on the results presented in Figure 5, the lowest coefficient of friction was observed for the S5-P/D_t=2 configuration at a Re of 30000. In this configuration, the f increased by 1.11 times compared to the smooth tube. On the other hand, the highest f, which was 0.04458, was found for the S4-P/D_t=1 model at the lowest Re of 5000.

3.3. Overall enhancement

In thermal systems, the implementation of heat transfer enhancement techniques is aimed at improving heat transfer, but it often comes at the cost of increased pressure drop. Recognizing that an increase in pressure drop is not a desirable outcome, Webb R.L. [47] introduced the coefficient of thermohydraulic performance. This coefficient serves as a metric to express the net energy gain in

systems where heat transfer improvement techniques are applied, offering a comprehensive assessment that considers both enhanced heat transfer and the associated increase in pressure drop.

As depicted in Figure 6, the thermohydraulic coefficient of performance for configurations employing hybrid nanofluid and circular dimple is consistently above 1. This observation suggests that the applied method is thermally and hydraulically advantageous. A coefficient of performance above 1 indicates that, despite the increase in pressure drop associated with the heat transfer enhancement techniques, the net energy gain in terms of improved heat transfer outweighs the added hydraulic losses, making the overall system more efficient.

The thermo-hydraulic results exhibit a decreasing trend with an increase in Re. Consequently, higher overall enhancement is achieved at lower Re, as the pressure drop becomes more pronounced at higher Re. Specifically, configurations with P/D_t=1 demonstrate significantly better performance values, while P/D_t=2 configurations, as anticipated, exhibit relatively lower performance.

The highest thermo-hydraulic coefficient of performance was achieved by the S5-P/D_t=1 configuration, reaching 1.35 at the lowest Re. In contrast, for the P/D_t=2 configuration within the same fluid model, this value was slightly lower at 1.32. On the other hand, the lowest performance value, amounting to 1.16, was observed at the highest Re for the S4- P/Dt =2 model. These results indicate variations in performance based on different configurations and Re, with the S5-P/Dt=1 configuration exhibiting the most favorable thermo-hydraulic performance under the specified conditions.

4. Conclusions

In conclusion, the numerical study delved into the thermal and hydraulic performance of heat exchanger configurations employing hybrid nanofluids and circular dimples. The findings offer valuable insights into various
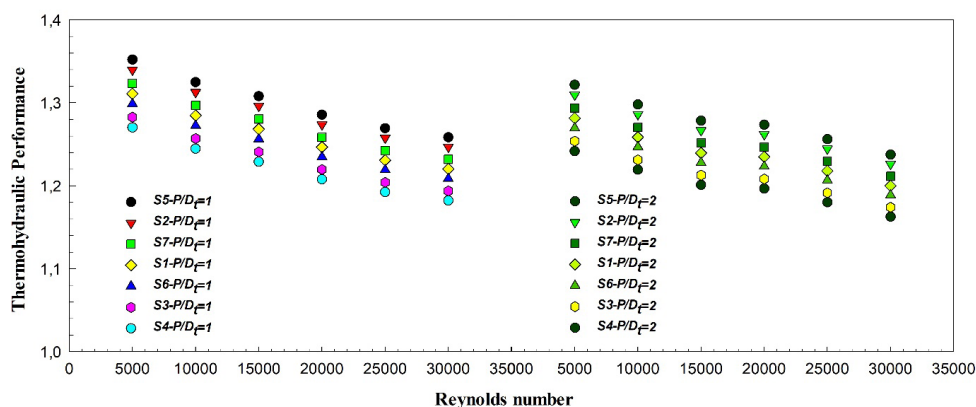

Figure 6. Distrubution of thermo-hydraulic performance versus Re for all configurations

parameters, shedding light on the effectiveness of heat transfer enhancement techniques.

- The ascending trend of Nu with increasing Reynolds number was consistently evident across all configurations, with the volumetric ratio of the hybrid nanofluid demonstrating a positive correlation, and circular dimples contributing to enhanced heat transfer. Specifically, the S5-*P/Dt*=1 configuration emerged as the most thermally favorable, showcasing superior thermal characteristics attributable to its unique fluid composition and the implementation of circular dimples with a shorter distance.

- Examining variations in the friction coefficient, the S5-*P/Dt*=2 configuration at Reynolds number 30000 yielded the lowest coefficient, albeit 1.11 times higher than the smooth tube. Conversely, the highest friction coefficient of 0.04458 was observed for the S4-*P/Dt*=1 model at the lowest Reynolds number of 5000.

- The thermohydraulic coefficient of performance consistently exceeded 1, indicating thermal and hydraulic advantages in configurations employing hybrid nanofluids and circular dimples. This signifies that, despite an associated increase in pressure drop, the net energy gain from improved heat transfer outweighs hydraulic losses.

- In terms of optimal performance, the S5-*P/Dt* =1 configuration demonstrated the highest thermohydraulic coefficient at 1.35, whereas the *P/Dt* =2 variation within the same fluid model exhibited a slightly lower value of 1.32. The lowest performance, amounting to 1.16, was observed at the highest Reynolds number for the S4-*P/Dt* =2 model.

- This comprehensive analysis offers significant insights into the intricate interplay of parameters, providing valuable guidance for the design and optimization of thermal systems employing hybrid nanofluids and circular dimples.

Nomenclature

c_p specific heat, j/kgK

f friction factor

FE_3O_4 Iron oxide

GnP Graphene nanoplatelet

h convective heat transfer coefficient, W/m²K

k thermal conductivity, W/mK

$MWCNT$ Multi-walled carbon nanotube

Nu Nusselt number

P pitch length, mm

Pr Prandtl number

q heat flux, W/m²

Q rate of heat transfer, W

r radius of the tube, mm

Re Reynolds number

T temperature, K

V average velocity, m/s

ΔP pressure drop, Pa

Greek symbols

ρ density, kg/m³

μ dynamic viscosity, kg/ms

ϕ volume concentration, %

Subscripts

f fluid

nf nanofluid

hnf hybrid nanofluid

$Thnf$ ternary hybrid nanofluid

b base

Rererences

[1] Shanthi, R., Anandan, S., & Ramalingam, V. (2012). Heat transfer enhancement using nanofluids: An overview. Thermal Science, 16(2): 423–444. doi:10.2298/tsci110201003s

[2] Gürdal, M., Pazarlıoğlu, H. K., Tekir, M., Arslan, K., & Gedik, E. (2022). Numerical investigation on turbulent flow and heat transfer characteristics of Ferro-nanofluid flowing in dimpled tube under magnetic field effect. Applied Thermal Engineering, 200: 117655. https://doi.org/10.1016/j.applthermaleng.2021.117655

[3] Dewan, A., Mahanta, P., Raju, K. S., & Kumar, P. S. (2004). Review of passive heat transfer augmentation techniques. Proceedings of the Institution of Mechanical Engineers, Part A: Journal of Power and Energy. 218(7): 509–527. doi:10.1243/0957650042456953

[4] Sheikholeslami, M., Gorji-Bandpy, M., & Ganji, D. D. (2015). Review of heat transfer enhancement methods: Focus on passive

methods using swirl flow devices. Renewable and Sustainable Energy Reviews, 49: 444–469. doi:10.1016/j.rser.2015.04.113

[5] Léal, L., Miscevic, M., Lavieille, P., Amokrane, M., Pigache, F., Topin, F., … Tadrist, L. (2013). An overview of heat transfer enhancement methods and new perspectives: Focus on active methods using electroactive materials. International Journal of Heat and Mass Transfer, 61:505-524. doi:10.1016/j.ijheatmasstransfer.2013.01.083

[6] Mousavi Ajarostaghi, S. S., Zaboli, M., Javadi, H., Badenes, B., & Urchueguia, J. F. (2022). A review of recent passive heat transfer enhancement methods. Energies, 15(3): 986. https://doi.org/10.3390/en15030986

[7] Kiwan, S., & Al-Nimr, M. A. (2001). Using Porous Fins for Heat Transfer Enhancement. Journal of Heat Transfer, 123(4), 790. doi:10.1115/1.1371922

[8] Pavel, B. I., & Mohamad, A. A. (2004). An experimental and numerical study on heat transfer enhancement for gas heat exchangers fitted with porous media. International Journal of Heat and Mass Transfer, 47(23): 4939–4952. doi:10.1016/j.ijheatmasstransfer.2004.06.014

[9] Wang, B., Hong, Y., Hou, X., Xu, Z., Wang, P., Fang, X., & Ruan, X. (2015). Numerical configuration design and investigation of heat transfer enhancement in pipes filled with gradient porous materials. Energy Conversion and Management, 105: 206–215. doi:10.1016/j.enconman.2015.07.064

[10] Pethkool, S., Eiamsa-ard, S., Kwankaomeng, S., & Promvonge, P. (2011). Turbulent heat transfer enhancement in a heat exchanger using helically corrugated tube. International Communications in Heat and Mass Transfer, 38(3): 340–347. doi:10.1016/j.icheatmasstransfer.2010.11.014

[11] Kareem, Z. S., Mohd Jaafar, M. N., Lazim, T. M., Abdullah, S., & AbdulWahid, A. F. (2015). Heat transfer enhancement in two-start spirally corrugated tube. Alexandria Engineering Journal, 54(3): 415–422. doi:10.1016/j.aej.2015.04.001

[12] Kareem, Z. S., Mohd Jaafar, M. N., Lazim, T. M., Abdullah, S., & Abdulwahid, A. F. (2015). Passive heat transfer enhancement review in corrugation. Experimental Thermal and Fluid Science, 68: 22–38. doi:10.1016/j.expthermflusci.2015.04.012

[13] Kareem, Z. S., Abdullah, S., Lazim, T. M., Mohd Jaafar, M. N., & Abdul Wahid, A. F. (2015). Heat transfer enhancement in three-start spirally corrugated tube: Experimental and numerical study. Chemical Engineering Science, 134: 746.

[14] Nuntaphan, A., Vithayasai, S., Vorayos, N., Vorayos, N., & Kiatsiriroat, T. (2010). Use of oscillating heat pipe technique as an extended surface in wire-on-tube heat exchanger for heat transfer enhancement. International Communications in Heat and Mass Transfer, 37(3): 287–292. doi:10.1016/j.icheatmasstransfer.2009.11.006

[15] Nagarani, N., Mayilsamy, K., Murugesan, A., & Kumar, G. S. (2014). Review of the utilization of extended surfaces in heat transfer problems. Renewable and Sustainable Energy Reviews, 29: 604–613. doi:10.1016/j.rser.2013.08.068

[16] Yadav, V., Baghel, K., Kumar, R., & Kadam, S. T. (2016). Numerical investigation of heat transfer in extended surface microchannels. International Journal of Heat and Mass Transfer, 93: 612–622. doi:10.1016/j.ijheatmasstransfer.2015.10.023

[17] Bi, C., Tang, G. H., & Tao, W. Q. (2013). Heat transfer enhancement in mini-channel heat sinks with dimples and cylindrical grooves. Applied Thermal Engineering, 55(1-2): 121–132. doi:10.1016/j.applthermaleng.2013.03.007

[18] Turnow, J., Kornev, N., Isaev, S., & Hassel, E. (2010). Vortex mechanism of heat transfer enhancement in a channel with spherical and oval dimples. Heat and Mass Transfer, 47(3): 301–313. doi:10.1007/s00231-010-0720-5

[19] Huang, X., Yang, W., Ming, T., Shen, W., & Yu, X. (2017). Heat transfer enhancement on a microchannel heat sink with impinging jets and dimples. International Journal of Heat and Mass Transfer, 112: 113–124. doi:10.1016/j.ijheatmasstransfer.2017.04.078

[20] Huang, Z., Yu, G. L., Li, Z. Y., & Tao, W. Q. (2015). Numerical Study on Heat Transfer Enhancement in a Receiver Tube of Parabolic Trough Solar Collector with Dimples, Protrusions and Helical Fins. Energy Procedia, 69: 1306–1316. doi:10.1016/j.egypro.2015.03.149

[21] Xie, S., Liang, Z., Zhang, L., & Wang, Y. (2018). A numerical study on heat transfer enhancement and flow structure in an enhanced tube with cross ellipsoidal dimples. International Journal of Heat and Mass Transfer, 125: 434–444. doi:10.1016/j.ijheatmasstransfer.2018.04.106

[22] Tijing, L. D., Pak, B. C., Baek, B. J., & Lee, D. H. (2006). A study on heat transfer enhancement using straight and twisted internal fin inserts. International Communications in Heat and Mass Transfer, 33(6): 719–726. doi:10.1016/j.icheatmasstransfer.2006.02.006

[23] García, A., Vicente, P. G., & Viedma, A. (2005). Experimental study of heat transfer enhancement with wire coil inserts in laminar-transition-turbulent regimes at different Prandtl numbers. International Journal of Heat and Mass Transfer, 48(21-22): 4640–4651. doi:10.1016/j.ijheatmasstransfer.2005.04.024

[24] Eiamsa-ard, S., Wongcharee, K., Eiamsa-ard, P., & Thianpong, C. (2010). Heat transfer enhancement in a tube using delta-winglet twisted tape inserts. Applied Thermal Engineering, 30(4): 310–318. doi:10.1016/j.applthermaleng.2009.09.006

[25] Promvonge, P., & Eiamsa-ard, S. (2006). Heat transfer enhancement in a tube with combined conical-nozzle inserts and swirl generator. Energy Conversion and Management, 47(18-19): 2867–2882. doi:10.1016/j.enconman.2006.03.034

[26] Firoozi, A., Majidi, S., & Ameri, M. (2020). A numerical assessment of heat transfer and flow characteristics of nanofluid in tubes enhanced with a variety of dimple configurations. Thermal Science and Engineering Progress, 100578. doi:10.1016/j.tsep.2020.100578

[27] Akçay, S. (2021). Investigation of thermo-hydraulic performance of nanofluids in a zigzag channel with baffles. Adıyaman Üniversitesi Mühendislik Bilimleri Dergisi, 8 (15): 525-534.

[28] Akçay, S. (2023). Numerical analysis of hydraulic and thermal performance of al2o3-water nanofluid in a zigzag channel with central winglets. Gazi University Journal of Science, 36(1): 383-397.

[29] Vicente, P. G., Garcıa, A., & Viedma, A. (2002). Experimental study of mixed convection and pressure drop in helically dimpled tubes for laminar and transition flow. International Journal of Heat and Mass Transfer, 45(26): 5091–5105. doi:10.1016/s0017-9310(02)00215-6

[30] Vicente, P. G., Garcıa, A., & Viedma, A. (2004). Mixed convection heat transfer and isothermal pressure drop in corrugated tubes for laminar and transition flow. International Communications in Heat and Mass Transfer, 31(5): 651–662. doi:10.1016/s0735-1933(04)00052-1

[31] Zheng, N., Liu, P., Shan, F., Liu, Z., & Liu, W. (2017). Turbulent

flow and heat transfer enhancement in a heat exchanger tube fitted with novel discrete inclined grooves. International Journal of Thermal Sciences, 111: 289–300. doi:10.1016/j.ijthermalsci.2016.09.010

[32] Chen, J., Müller-Steinhagen, H., & Duffy, G. G. (2001). Heat transfer enhancement in dimpled tubes. Applied Thermal Engineering, 21(5): 535–547. doi:10.1016/s1359-4311(00)00067-3

[33] Piper, M., Zibart, A., Djakow, E., Springer, R., Homberg, W., & Kenig, E. Y. (2019). Heat transfer enhancement in pillow-plate heat exchangers with dimpled surfaces: a numerical study. Applied Thermal Engineering, 153:142-146. doi:10.1016/j.applthermaleng.2019.02.082

[34] Bi, C., Tang, G. H., & Tao, W. Q. (2013). Heat transfer enhancement in mini-channel heat sinks with dimples and cylindrical grooves. Applied Thermal Engineering, 55(1-2): 121–132. doi:10.1016/j.applthermaleng.2013.03.007

[35] Kabeel, A. E., Abou El Maaty, T., & El Samadony, Y. (2013). The effect of using nano-particles on corrugated plate heat exchanger performance. Applied Thermal Engineering, 52(1): 221–229. doi:10.1016/j.applthermaleng.2012.11.027

[36] Khairul, M. A., Alim, M. A., Mahbubul, I. M., Saidur, R., Hepbasli, A., & Hossain, A. (2014). Heat transfer performance and exergy analyses of a corrugated plate heat exchanger using metal oxide nanofluids. International Communications in Heat and Mass Transfer, 50: 8–14. doi:10.1016/j.icheatmasstransfer.2013.11.006

[37] Suresh, S., Chandrasekar, M., & handra Sekhar, S. (2011). Experimental studies on heat transfer and friction factor characteristics of CuO/water nanofluid under turbulent flow in a helically dimpled tube. Experimental Thermal and Fluid Science, 35(3): 542–549. doi:10.1016/j.expthermflusci.2010.12.008

[38] Ekiciler, R., & Samet Ali Çetinkaya, M. (2021). A comparative heat transfer study between monotype and hybrid nanofluid in a duct with various shapes of ribs. Thermal Science and Engineering Progress, 23: 100913. doi:10.1016/j.tsep.2021.100913

[39] Toghraie, D., Chaharsoghi, V. A., & Afrand, M. (2016). Measurement of thermal conductivity of ZnO–TiO2/EG hybrid nanofluid. Journal of Thermal Analysis and Calorimetry, 125(1): 527–535. doi:10.1007/s10973-016-5436-4

[40] Sundar, L. S., Singh, M. K., & Sousa, A. C. M. (2018). Turbulent heat transfer and friction factor of nanodiamond-nickel hybrid nanofluids flow in a tube: An experimental study. International Journal of Heat and Mass Transfer, 117: 223–234. doi:10.1016/j.ijheatmasstransfer.2017.09.109

[41] Khan, A., & Ali, M. (2022). Thermo-hydraulic behavior of alumina/silica hybrid nanofluids through a straight minichannel heat sink. Case Studies in Thermal Engineering, 31: 101838. https://doi.org/10.1016/j.csite.2022.101838

[42] Ahmed, F., Abir, M. A., Fuad, M., Akter, F., Bhowmik, P. K., Alam, S. B., & Kumar, D. (2021). Numerical investigation of the thermo-hydraulic performance of water-based nanofluids in a dimpled channel flow using Al2O3, CuO, and hybrid Al2O3–CuO as nanoparticles. Heat Transfer, 50(5): 5080–5105. doi:10.1002/htj.22116

[43] Mertaslan, O. M., & Keklikcioglu, O. (2024). Investigating heat exchanger tube performance: second law efficiency analysis of a novel combination of two heat transfer enhancement techniques. Journal of Thermal Analysis and Calorimetry. https://doi.org/10.1007/s10973-023-12842-6

[44] ANSYS, 2018. ANSYS Fluent Tutorial Guide, ANSYS Inc., Canonsburg.

[45] Gnielinski, V. (1976). New equations for heat and mass transfer in turbulent pipe and channel flow. International Chemical Engineering, 27; 359–368.

[46] Petukhov, B. S., Irvine, T. F., & Hartnett, J. P. (1970). Advances in heat transfer. Academic, New York, 6; 503–564.

[47] Webb, R. L. (1981). Performance evaluation criteria for use of enhanced heat transfer surfaces in heat exchanger design. International Journal of Heat and Mass Transfer, 24; 715–726.